Cationic Iridium Complexes with Chiral Dithioether Ligands: Synthesis, Characterisation and Reactivity under Hydrogenation Conditions

Leticia Flores-Santos,[a] Erika Martin,*[a] Ali Aghmiz,[b] Montserrat Diéguez,[b] Carmen Claver,[b] Anna M. Masdeu-Bultó,*[b] and Miguel Ángel Muñoz-Hernández[c]

Keywords: Chiral auxiliaries / S ligands / Iridium / Hydrides / Asymmetric catalysis

A series of cationic Ir^I complexes containing chiral dithioether ligands have been prepared in order to study the influence of the sulfur substituents and the metallacycle size on the acetamidoacrylate hydrogenation reaction. In the case of complexes **6**, **7** and **10**, a mixture of diastereomers is observed in solution due to the sulfur inversion processes. In contrast, this fluxional behaviour is efficiently controlled by using bicyclic ligands which inhibit the S-inversion in complexes **8** and **9**. The solid-state structure of complex **10b** shows only one diastereomer with the sulfur substituents in a relative *anti* disposition and in an overall configuration of $S_CS_CS_SS_S$ at the coordinated dithioether ligand. Iridium complexes containing seven- and six-membered metallacycles (**6b**–**d**, **7b**,c, **10a**,**b**) react with the substrate through S-ligand substitution, and the rate of this substitution is related to the position of the fluorine atom on the aromatic ring. On the contrary, complexes containing a *bis*metallacycle (**8** and **9**) are not displaced by the substrate. The catalytic hydrogenation activity of complexes **8** and **9** is analysed in terms of the high stability of the corresponding dihydride complexes (**13** and **14**). In both cases, only two of the four possible diastereomeric dihydride species are formed in solution.

Introduction

The study of chiral sulfur transition-metal complexes as asymmetric catalysts has notably increased during the last decades.[1,2] In particular, complexes containing thioether mixed-donor ligands such as the P,S-,[3–8] N,S-[9–17] and O,S-[18–22] donors have been successfully applied in asymmetric hydrogenation,[5,6,23] allylic substitutions[7–10,18] and enantioselective hydrosilylation of ketones.[4,23] In contrast, catalysts with chiral bidentate thioether ligands have been scarcely investigated,[24–32] although some have shown promising catalytic properties. In fact, we have recently shown that metal complexes with chiral dithioether ligands afford up to 81% *ee* in palladium-catalysed asymmetric allylic substitutions[24] and 68% *ee* in iridium-catalysed asymmetric hydrogenation reactions.[25,26]

Upon coordination to a metal, thioether ligands generate a stereogenic centre at the sulfur atom, whose close proximity to the metal coordination sphere may be advantageous for enantioinduction; however, these centres are not configurationally stable, since sulfur inversion has a low energy barrier. In the case of chiral dithioether complexes, the presence of two stereogenic centres at sulfur atoms, in addition to the carbon stereogenic centres at the ligand backbone, can lead to mixtures of diastereomers. The presence of mixtures of diasteromeric species and the difficulty to control their interconversion in solution have been regarded as a problem for asymmetric induction in catalytic reactions. In spite of this behaviour, enantioinductions have been improved when the configuration at the sulfur atom is controlled by steric effects.[24,31,32] Unfortunately, having few examples of S,S-homodonor ligands, which also differ considerably in their skeleton size and rigidity, makes it difficult to elucidate the structure-performance relationship.

In order to understand the influence of structural and electronic factors on the reactivity of chiral dithioether-containing catalysts, in the present work we prepared a series of cationic iridium complexes with chiral dithioether ligands **1**–**5** (Figure 1) derived from L-(+)-diethyltartrate[33] and (2*R*,4*R*)-2,4-pentanediol.[34] These ligands were selected in order to study electronic and ring size effects and sulfur inversion control, by the following strategies: (i) introduction of fluorine atoms at *ortho*- *meta*- or *para*- positions of a thioether aromatic ring in order to change the donor/acceptor electronic properties of sulfur atoms (ligands **1a–c** and **2a**–**c**); (ii) evaluation of two ring sizes to tune the rigidity of the molecular backbone (ligands **1a**–**d** and **2a**–**c** vs.

[a] Departamento de Química Inorgánica, Facultad de Química, Universidad Nacional Autónoma de México, Cd. Universitaria, 04510 México DF, México
Fax: +52-55-5622-3720
E-mail: erikam@servidor.unam.mx
[b] Departament de Química Física i Inorgànica, Universitat Rovira i Virgili,
c/Marcel·lí Domingo s/n, 43005 Tarragona, Spain
Fax: +34 977-559563
E-mail: masdeu@quimica.urv.es
[c] Centro de Investigaciones Químicas, Universidad Autónoma del Estado de Morelos,
Av. Universidad 1001 Col. Chamilpa, Cuernavaca, México
Fax: +52-77-7329-7998
E-mail: mamund2@ciq.uaem.mx

5); (iii) effective stereocontrol at sulfur atoms in metal intermediates by using cyclic chiral thioether ligands which eliminate pyramidal inversion and also allow a backbone rigidity modulation (ligands **3** and **4**).

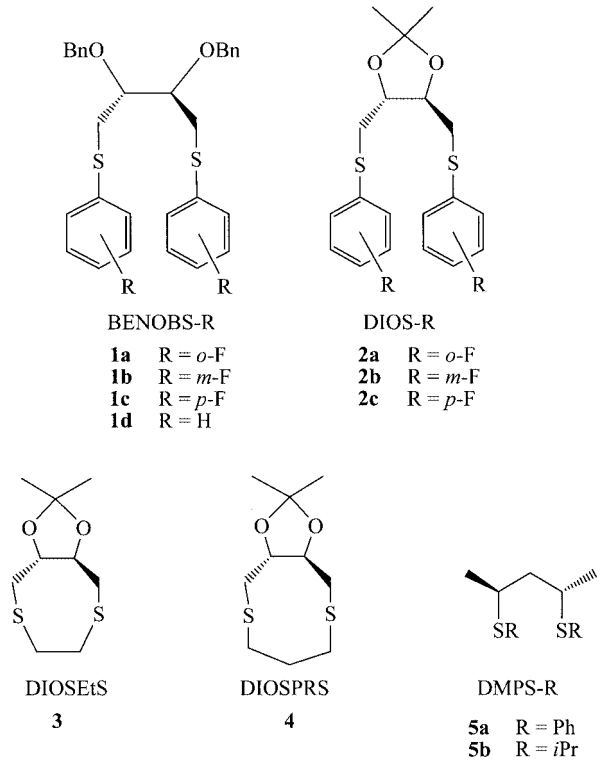

Figure 1. Dithioether ligands **1–5**.

The reactivity of the synthesised complexes [Ir(dithioether)(cod)]BF_4 towards acrylic acid derivatives and dihydrogen is discussed in relation to the activity and selectivity observed under catalytic hydrogenation conditions.

Results and Discussion

Iridium Complexes [Ir(cod)(dithioether)]BF_4

Ligands **3**, **4** and **5a**,**b** reacted with dichloromethane solutions of [Ir(cod)$_2$]BF_4 to form the corresponding [Ir(cod)(dithioether)]BF_4 complexes **8**, **9** and **10a**,**b** by cod substitution (Scheme 1). The complexes were isolated as relatively air-stable, yellow or orange solids by addition of hexane or diethyl ether with yields ranging from 50 to 99%. In contrast, ligands **1a–d** and **2a–c** did not react with dichloromethane solutions of [Ir(cod)$_2$]BF_4 unless hydrogen was bubbled through the solution to reduce cod and promote its substitution. These results can be rationalised according to the lower stability of the seven-membered metallacycle formed in the case of ligands **1** and **2**. A similar behaviour was observed for the non-fluorinated derivative of ligands **2**.[25] In the case of ligands **3** and **4**, the generation of [7,5]- and [7,6]-membered rings, respectively, increases the chelate stability. Dithioethers **1a** and **2a** did not form the iridium complexes, probably because of steric hindrance in addition to the electron-withdrawing effect of the *ortho*-fluoro substitution.

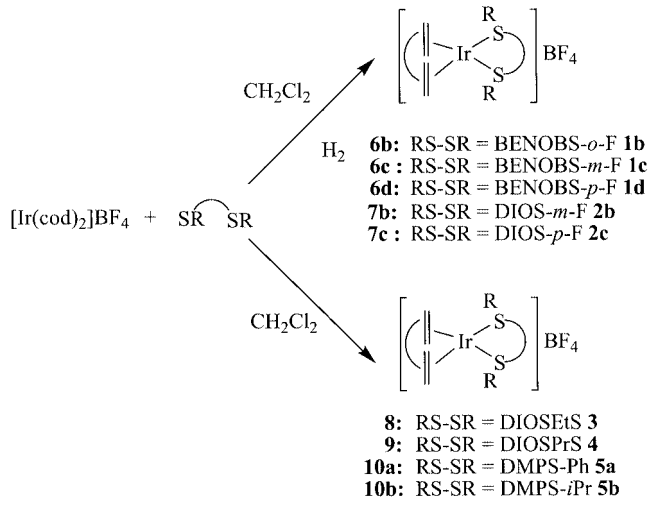

Scheme 1. Syntheses of complexes **6–10**.

FAB mass spectra confirmed the formation of the mononuclear species in all cases. Complexes were characterised in solution by ^1H and ^{13}C NMR spectroscopy. ^{19}F NMR spectroscopy was also used for complexes **6b**,**c** and **7b**,**c**. The full assignment of ^1H and ^{13}C NMR parameters was performed by using homo- and heteronuclear two-dimensional spectroscopy techniques (^1H,^1H-COSY, HETCOR and NOESY).

The coordination of the dithioether ligands to the metal generates a stereogenic centre at each sulfur atom. Therefore, a mixture of diastereomers with different spatial arrangements of the sulfur substituents and conformations of the chelate ring could exist in solution (Figure 2). Taking into account that ligands **1** and **2** have absolute *RR*-configuration at their asymmetric carbon centres and two possible configurations at the sulfur atoms, three diastereomers could be formed: $R_CR_CR_SR_S$ and $R_CR_CS_SS_S$ (both attributed to the *anti* isomers) and $R_CR_CR_SS_S$ or $R_CR_CS_SR_S$ (corresponding to the *syn* isomer). This analysis applies also for complexes with ligands **5**, which have absolute *SS* configuration at their asymmetric carbon centres, therefore three possible diastereomers, $S_CS_CR_SR_S$ and $S_CS_CS_SS_S$ (*anti* isomers), and $S_CS_CR_SS_S$ or $S_CS_CS_SR_S$ (*syn* isomer) can be formed. In contrast, for complexes containing ligands **3** and **4**, there is only one possible *syn* isomer with $R_CR_CR_SS_S$ or $R_CR_CS_SR_S$ configuration, since the inversion at both sulfur atoms is inhibited.

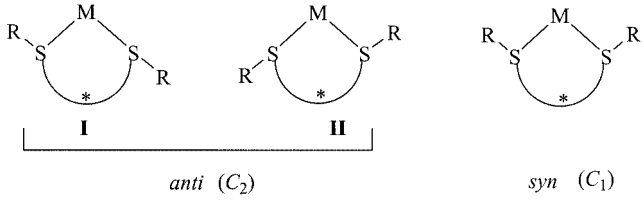

Figure 2. Possible diastereomers for metal complexes with ligands **1–5**.

In fact, variable temperature NMR studies (down to –80 °C) performed on complexes **8** and **9** are in accordance with the presence of only one diastereomer in solution, which corresponds to a C_1-symmetry molecule with $R_CR_CR_SS_S$ configuration. Full assignment of ^{1}H and ^{13}C spectra was achieved by homo- and heteronuclear 2D NMR techniques and the conformation of both rings was determined by using NOE experiments (Figure 3). The seven-membered ring has a twisted chair conformation in both complexes. The second ring is either a five-membered chelate ring with an envelope conformation in **8** (NOE contact between H^4 with H^1 and H^2) or a six-membered ring with a chair conformation in **9** (NOE contact between H^1 and H^7).

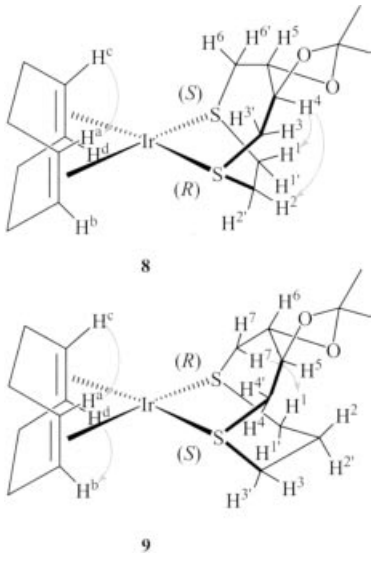

Figure 3. Structures proposed for complexes **8** and **9** showing the NOE contacts.

For complexes **10a**,**b** containing a six-membered metallacycle, variable temperature ^{1}H NMR spectra (–40 to +25 °C) exhibited patterns corresponding to the presence of only one species with C_2 symmetry, which may be attributed to one of the two possible *anti* diastereomers $S_SS_CS_CS_CS_S$ or $R_SS_CS_CR_S$ with equatorial–equatorial or axial–axial conformations, or to the chair equatorial–axial conformers interchanging fast in solution. VT NMR spectra of **10b** in CD_2Cl_2 were invariant in the temperature range studied. NOE experiments suggested that an equatorial–equatorial species was likely to be present in solution; nevertheless, the possibility of rapid equilibration with other species could not be discarded. Moreover, the structure in the solid state of **10b**, determined by X-ray diffraction (see following section), confirmed that the sulfur substituents were *anti* with an equatorial–axial disposition.

The ^{1}H and ^{19}F NMR spectra of complexes **6b**,**c** and **7b**,**c** show in all cases broad signals at room temperature. It is interesting to note that the chemical shifts of the cod methynic protons are not sensitive to the position of the fluoro substituent on the dithioether ligands. Nevertheless, the reactivity towards acrylic acid derivatives depends on the position of the fluorine atom in the aromatic ring.

The ^{13}C NMR spectra for complexes **6b–d** showed only two signals for cod methylenic carbons and two signals for cod methynic carbons, which can be attributed to the presence of only one *anti* diastereomer or a fast exchange between both *anti* diastereomers. However, the ^{19}F NMR experiments in the temperature range of +30 °C to –60 °C show two different signals for complexes **6b** and **6c** in the ratios 10:6 and 10:9.1, respectively, proving the presence of two *anti* diastereomers in solution (**I** and **II**). The rate of isomer interconversion for complex **6b** was very low and invariant in the temperature range studied ($k = 1.10^{-3}$ s^{-1}) [35], and for complex **6c** the rate could not be calculated, since no significant change in the shape of the spectra was observed in the same range of temperatures. Although no splitting of signals in ^{1}H and ^{13}C NMR spectra was observed for complex **6d**, by analogy with **6c**,**d**, two diastereomers could also be present in solution.

In the case of complexes **7b** and **7c**, two isomers, **I** and **II**, were also detected at low temperature. The exchange rates ranged from 5.26×10^2 s^{-1} (at –60 °C) to 1.22×10^4 s^{-1} (at 30 °C) for **7b** and from 8.22×10^2 s^{-1} (–60 °C) to 5×10^4 s^{-1} (30 °C) for **7c**. The values of the Gibbs activation energy ($\Delta G^{\neq}$, evaluated by the Eyring equation) are 50.4 ± 1.0 kJ mol^{-1} for **7b** and 48.1 ± 1.3 kJ mol^{-1} for **7c**, and are in the range reported for sulfur inversion in thioether complexes.[36,37] Therefore, the dynamic behaviour in solution of **7b** and **7c** is independent of the position of the fluorine atom in the aromatic ring.

Crystal Structure of [Ir(cod)(5b)]BF$_4$ (10b)

Single crystals of **10b** suitable for X-ray diffraction were obtained by slow diffusion of *n*-hexane into an ethyl acetate solution of the complex. The cationic structure is shown in Figure 4, and selected bond lengths and angles are listed in Table 1. The iridium atom shows a slightly distorted square-planar environment. The sulfur atoms are in a *cis* configuration and the cyclooctadiene ligand occupies the other two coordination sites. For the latter ligand, using the centroids of the C12–C13 and C16–C17 double bonds, X1a and X1b, respectively, a twist of 4.8° of the dihedral planes S1–Ir1–S2 and X1a–Ir1–X1b is found. A similar situation was observed for the Ir complex [Ir(cod){C[P(S)(Ph)$_2$]$_3$}],[38] which showed a twist of 9.0°. The distortion is also evident from the deviation from 90° observed in the following bond angles: X1a–Ir1–S1 86.8°, X1b–Ir1–S2 99.6° and X1a–Ir1–X1b 85.6°, which is more pronounced than in [Ir(cod)-{[P(S)(Ph)$_2$]$_3$C}] (89.5, 88.3 and 87.5°, respectively)[38] and the Rh complex [Rh(cod){CH[P(S)(Ph)$_2$]$_2$}] (86.4, 88.3 and 86.7°, respectively).[39] The Ir–S and Ir–C average bond lengths [2.3537(19) and 2.131(9) Å, respectively] are in the range reported for related Ir^{I} complexes.[38,40,41] Furthermore, similar Ir–S distances were reported for Ir^{I} cyclooctadiene complexes with thiolate bridging ligands.[42,43] The average angle C–S–Ir [110.0(3)°] is close to the tetrahedral angle, indicating sp^3 hybridization at the sulfur atom.

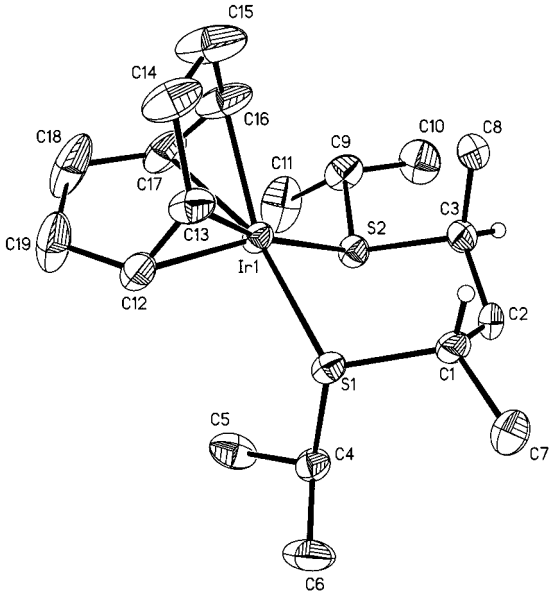

Figure 4. ORTEP representation (50% probability) of iridium complex **10b**. Hydrogen atoms and BF_4^- are omitted.

Table 1. Selected bond lengths [Å] and angles [°] for complex **10b**.

Bond lengths	[Å]	Bond angles	[°]
Ir(1)–C(16)	2.116(11)	C(16)–Ir(1)–C(12)	95.5(4)
Ir(1)–C(12)	2.126(8)	C(17)–Ir(1)–C(13)	88.4(4)
Ir(1)–C(17)	2.141(9)	C(16)–Ir(1)–S(2)	98.6(3)
Ir(1)–C(13)	2.141(8)	C(17)–Ir(1)–S(2)	99.6(3)
Ir(1)–S(2)	2.344(2)	C(12)–Ir(1)–S(1)	85.9(2)
Ir(1)–S(1)	2.3633(18)	C(13)–Ir(1)–S(1)	87.9(2)
		S(2)–Ir(1)–S(1)	88.18(8)
		C(1)–S(1)–C(4)	105.0(4)
		C(1)–S(1)–Ir(1)	108.3(3)
		C(4)–S(1)–Ir(1)	111.3(3)
		C(3)–S(2)–C(9)	105.4(4)
		C(3)–S(2)–Ir(1)	104.4(3)
		C(9)–S(2)–Ir(1)	116.1(3)

The solid structure shows only one diastereomer with the sulfur substituents in a relative *anti* disposition. The metallacycle adopts a chair conformation with an overall configuration $S_C S_C S_S S_S$.

Catalytic Experiments and Reactivity of the Iridium Complexes

The catalytic activity of iridium complexes **6b**–**d**, **7b**,**c**, **8**, **9**, **10a**,**b** in the hydrogenation of acrylic acid derivative **11a** at 25 °C and 1 atm of hydrogen pressure was examined (Scheme 2).

All catalyst precursors show low conversions even at 12 h of reaction (Figure 5). Regarding the influence of the fluoro-substitution on the aromatic ring, the *meta*-fluoro derivatives **6b** and **7b** showed higher conversion than their analogous *para*-fluoro derivatives **6c** and **7c**, in the same reaction time. The complex **6d** without the fluoro-substituted ligand showed higher conversion than the *meta*- and *para*-fluoro complexes **6b** and **6c**.

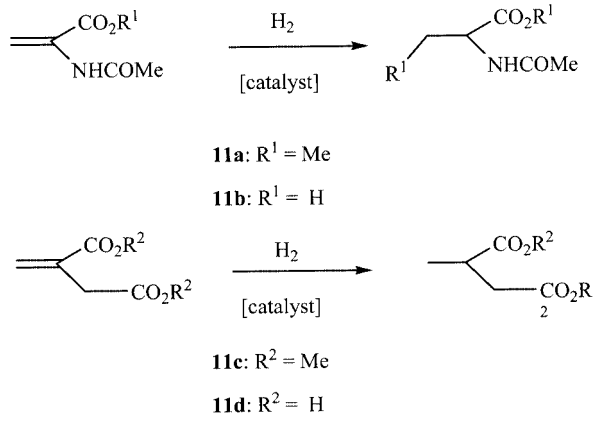

Scheme 2. Hydrogenation of acrylic acid derivatives **11a**–**d**.

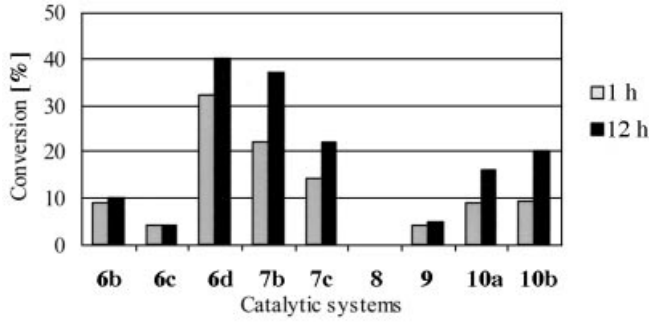

Figure 5. Catalytic hydrogenation of methyl acetamidoacrylate (**11a**) by using dithioether iridium complexes. Conditions: [{Ir(cod)L}BF_4] = 4.3 mM, [Substrate] = 175 mM, T = 25 °C and $p(H_2)$ = 1 atm.

The activity is also modified by the dithioether skeleton; complexes **7b**,**c** provided higher conversion than **6b**,**c** and complex **10a**, with a smaller six-membered metallacycle, showed lower conversion than the seven-membered chelate complex **6d**. Finally, complexes **8** and **9**, which contain metallabicycles, provided less active catalytic systems. In all cases, the enantioinduction was practically nonexistent.

These catalytic results can be explained in terms of the stability of the complexes. Catalytic systems **6**, **7** and **10** decomposed gradually during the catalytic reaction to form Ir^0 with the consequent loss of the chiral ligand. This was confirmed for the fluorinated precursors (**6b**,**c** and **7b**,**c**) by analysis of the catalytic mixture at the end of the hydrogenation reactions through ^{19}F NMR spectroscopy, which showed the presence of the free ligand as a distinct species. The decoordination of the dithioether ligands is promoted by substrate coordination, since the addition of **11a** to dichloromethane solutions of complexes **6**, **7** and **10** under nitrogen generates free dithioether ligands and [Ir(**11a**)(cod)]$^+$, detected by ^{19}F NMR spectroscopy or by ^1H and ^{13}C NMR.

In an attempt to recoordinate the dithioether ligand by forcing cod reduction, H_2 was bubbled into a solution containing **6b** and **11a**, but the signal of the free dithioether

remained unaltered, and the formation of metallic iridium was observed.

For purposes of comparison, the catalytic activity of complex $[Ir(cod)_2]^+$ (**12**) was studied under the same catalytic conditions and was found to be the highest (45% conversion at 1 h). Since the conversion obtained with **12** is higher than that found with the dithioether complexes and it has been demonstrated that these dithioether ligands are replaced by the substrate to yield $[Ir(\mathbf{11a})(cod)]^+$, the increasing conversion can be related to a higher rate of dithioether substitution. Thus, the less active systems are those in which the rate of substitution is lower, suggesting that the dithioether ligand is more strongly coordinated to the metal. Consequently, in the case of seven-membered complexes, catalytic precursors **6** lead to more active systems probably because of the formation of weaker M–S bonds. The same situation is observed when the more stable six-membered complex **10a** is compared with the seven-membered complex **6b**. Concerning the electronic factors, the lower activity of the fluorinated systems may be related to a stronger M–S interaction due to an enhancement of the π-acceptor ability of these ligands.

In contrast to the above-mentioned behaviour, bicyclic systems **8** and **9** do not decompose to Ir^0 under catalytic conditions, and the dithioether ligands are not replaced by substrate **11a**. Therefore, the catalytic hydrogenation of **11b**–**d** was studied by using **8** and **9**. For these substrates, the conversions ranged from modest to low and only for the acid substrates **11b** and **11d**, the *ee* reached up to 15% (*R*), with **8** as catalyst precursor. In order to understand the catalytic performance of these *bis*metallacycles, we studied the species formed in the presence of hydrogen.

Reactivity of Complexes 8 and 9 with Hydrogen

Complexes **8** and **9** reacted with H_2 at –70 °C to form the corresponding dihydride species $[Ir(H)_2(\mathbf{8})(cod)]BF_4$ (**13**) and $[Ir(H)_2(\mathbf{9})(cod)]BF_4$ (**14**) (Scheme 3). Similar reactivity was reported for other dithioether iridium complexes.[25,26]

$$[Ir(COD)(L)]BF_4 + H_2 \longrightarrow [Ir(H)_2(COD)(L)]BF_4$$

8: L = DIOSEtS **3** — **13**: L = DIOSEtS **3**
9: L = DIOSPrS **4** — **14**: L = DIOSPrS **4**

Scheme 3. Reaction of complexes **8** and **9** with H_2.

Taking into account the two different faces of the coordination plane (named seven-membered- and five-membered ring faces) four diastereomers can be formed (Figure 6).

The hydride region of the ^1H NMR spectra of complex **13** showed four signals at –70 °C which were attributed to the presence of two different isomers: a major isomer (δ = –11.37 and –13.83 ppm) and a minor one (δ = –11.56 and –13.78 ppm) in a 5:3 ratio. The measurement of relaxation times, T_1 (see Experimental Section), confirmed the formation of "classical hydride ligands".[44–48] Moreover, signals at δ = –11.37 and –11.56 ppm showed similar T_1 values (0.31 s) and the same was observed for T_1 values (0.2 s) of

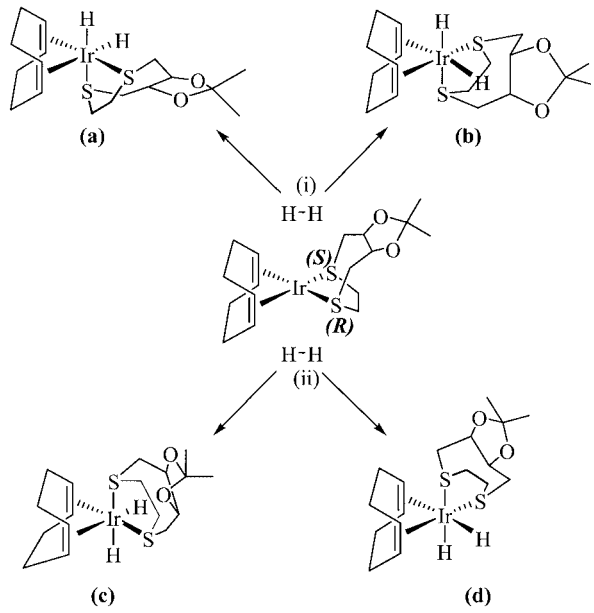

Figure 6. Attack of H_2 (i) through the "upper" seven-membered ring face with displacement of the (a) S_S (**13-I**) and (b) S_R atoms (**13-II**); (ii) through the "lower" five-membered ring face with displacement of the (c) S_S (**13-III**) and (d) S_R (**13-IV**) atoms.

signals at δ = –13.83 and –13.78 ppm, suggesting similar chemical environments for each couple sharing equal T_1 values.

NOE experiments allowed identification of the major isomer as **13-I**, formed by the attack of H_2 through the seven-membered ring face with displacement of the sulfur with absolute *S* configuration (Figure 7). In particular, NOE contacts between the methynic proton H^5 with $H^{3'}$ and the hydride ligand H^f, indicated the proximity of the seven-membered ring face to the hydride ligand. The methynic proton H^4 showed contacts with the ethyl protons $H^1$and H^2. The minor isomer corresponds to isomer **13-II**, formed also by the attack of H_2 through the seven-membered ring face but with displacement of the sulfur with absolute *R* configuration. The NOE contacts H^f–H^5, H^2–H^4–H^1 and H^b-$H^{3'}$ allowed determination of the minor isomer structure.

The dihydride complexes **13-I** and **13-II** were very stable; the hydride signals remained in the ^1H NMR spectra up to 25 °C after 24 h. The high stability of these complexes may account for the very low activity of **8** in the hydrogenation of acrylic acid derivatives. Although the oxidative addition takes place readily at –70 °C, the 1,2-insertion of the hydride ligands in the M-alkene (cod) bond to hydrogenate the cod ligand is very slow.

Similar results were obtained in the reactivity study of complex **9** with H_2 to form the dihydride complex **14**. The ^1H NMR in the hydride region also showed four signals corresponding to two isomers in a 5:3 ratio. In this case, the NOE contacts suggested that hydrogen attack also takes place through the seven-membered ring face for both isomers. The structure assignment of the major and minor isomers was not possible because the hydride NOE signals

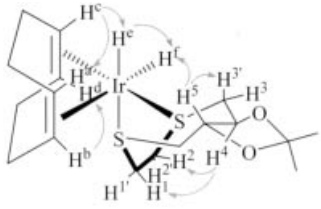

13-I

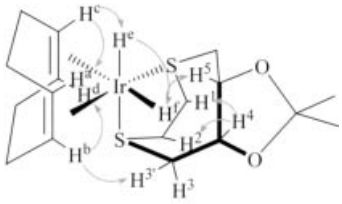

13-II

Figure 7. Representation of complexes of **13-I** and **13-II**, showing the NOE contacts.

were superimposed. Upon increasing the temperature up to 0 °C, the hydride signals disappeared, and both signals of cyclooctane and complex **9** were observed. This corresponds to two parallel reactions, the hydrogenation of cod and the reversible reductive elimination of H_2.

As has been shown, the approach of dihydrogen to complexes **8** and **9** takes place through the seven-membered ring face, which is presumably the more hindered. Nevertheless, upon formation of the dihydride complex, the reorganization of the dithioether cyclic ligand leads to a less hindered structure than when the approach is through the five- (for complex **8**) or six- (for complex **9**) -membered ring face. In this latter case, the bicyclic moiety of the resulting structure would be bent towards the cod coordinated ligand while in the other case, this fragment is launched outside the coordination sphere (Figure 6), which may favour the formation of the observed isomers. The low enantioselectivity obtained with both systems is probably related to the formation of different dihydrido complexes in solution.

Conclusion

Cationic iridium(I) complexes containing chiral dithioether ligands were prepared and their fluxional behaviour in solution was efficiently controlled by using bicyclic ligands, which form configurationally stable sulfur stereocentres upon coordination to the metal. The systematic study of the reactivity of these complexes allowed to establish that: (i) seven-membered chelating ligands are displaced in all cases by methyl acetoamidoacrylate to form the species $[Ir(substrate)(cod)]^+$, which is responsible for the catalytic activity in the hydrogenation of this substrate; (ii) the position of the fluorine atoms in the aromatic rings affects the substitution rate of the dithioether, thus modifying the catalytic activity directly; (iii) the dithioether substitution does not occur in the more rigid complexes containing cyclic dithioligands; however, these systems show poor activities and enantioselectivities; (iv) the low activity of the *bis*-metallacycles is directly related to the high stability of the corresponding dihydride species; (v) only two diastereomeric dihydride species (5:3) are formed in both cases; (vi) in the *bis*metallacycle systems the enantioinduction is slightly improved using the more rigid [7,5]- in comparison to the [7,6]-*bis*metallacycle.

Experimental Section

General Remarks: All iridium complexes were prepared by standard Schlenk techniques under nitrogen. The complex $[Ir(cod)_2]BF_4$ was prepared by methods described in the literature.[49] The syntheses of ligands **1a–d**, **2a–c**, **3** and **4** were reported previously.[33] The syntheses of ligands **5a** and **5b** will be described elsewhere.[34] Solvents were dried over standard drying agents and were freshly distilled and deoxygenated prior to use. All other reagents were used as commercially supplied. ^1H, ^{13}C, and ^{19}F NMR spectra were measured with Varian 300 or 400 MHz spectrometers operating at 300 or 400 MHz (^1H), 75 or 100 MHz (^{13}C), 282 or 376 MHz (^{19}F). Chemical shifts are relative to TMS δ = 0 ppm (^1H), CD_2Cl_2 δ = 55 ppm (^{13}C) and $CFCl_3$ δ = 0 ppm (^{19}F). All species were studied in deuterated dichloromethane unless otherwise indicated. Infrared spectra were measured with a Nicolet AVATAR 320 FT-IR spectrometer. Electronic Impact and FAB^+ mass spectra were recorded with a Jeol SX102A inverse geometry spectrometer and VG Autospect using a 3-nitrobenzyl alcohol matrix. Elemental analyses were performed with an AE FISONS CHNS-0 equipment or a Carlo–Erba EA-1108 microanalyser. Gas chromatography analyses were performed with a Hewlett–Packard 5890A instrument. Enantiomeric excesses (*ee*) were determined with a fused silica capillary column Permabond L-Chirasil-Val (25 m × 0.25 mm) for substrates **11a**,**b**, and Chiraldex-G-TA (30 m × 0.25 mm) for substrates **11c**,**d**.

Synthesis of Complexes [Ir(cod)(dithioether)]BF_4 (dithioether = 1b–d, 2b,c, 3–5)

Procedure A: A solution of the corresponding ligand (**1b–d, 2b**,**c**, 0.08 mmol) in dichloromethane (3 mL) was added to a solution of $[Ir(cod)_2]BF_4$ (40 mg, 0.08 mmol) in dichloromethane (5 mL) under nitrogen. The solution was stirred for 30 min, and then hydrogen was bubbled into the solution for 15 s in order to hydrogenate the 1,5-cyclooctadiene ligand and coordinate the dithioether to iridium. The solution was filtered to remove Ir^0, and the solvent was evaporated. The residue was thoroughly washed with hexane and recrystallised from dichloromethane/hexane to yield the products as yellow microcrystalline solids.

[Ir(cod)(1b)]BF_4 (6b): Colour: yellow; yield: 33.5 mg, 46%. IR [KBr (cm^{-1})]: (ν_{B-F}) 1064 (s). ^1H NMR (400 MHz): δ = 7.59 (m, 18 H, H_{ar}), 4.87 (m, 4 H, CH_2–C_6H_5), 4.19 (m, 2 H, CH), 3.95 (m, 4 H, CH_2), 3.82 (m, 4 H, CH cod), 2.3 (m, 2 H, CH_2 cod), 2.24 (m, 2 H, CH_2 cod), 1.81 (m, 2 H, CH_2 cod), 1.7 (m, 2 H, CH_2 cod) ppm. $^{13}C\{^1H\}$ NMR (100 MHz): δ = 162.83 (Ci-F, $J_{C,F}$ = 250.4), 137.16 (Ci-S), 131.66 (Ci), 129.2 (C_m-S), 128.9 (C_o), 128.7 (C_p), 128.56 (C_m), 118.19 (C_o–S, C*p*-S), 75.79 (CH), 74.65 (CH cod), 73.97 (CH cod), 73.67 (CH_2–C_6H_5), 31.14 (CH_2 cod), 31.08 (CH_2 cod), 29.46 (CH_2) ppm. ^{19}F NMR (376 MHz, –60 °C): δ = –109.45 (m, **6b-I**), –111.77 (m, **6b-II**) ppm; **6b-I**/**6b-II** = 5:3. FAB^+: *m*/*z* (%) = 823 ($M–BF_4$). $C_{38}H_{40}BF_6IrO_2S_2$ (909.88): calcd. C 50.16, H 4.43, S 7.05; found C 49.74, H 4.40, S 7.00.

[Ir(cod)(1c)]BF_4 (6c): Colour: yellow; yield: 26.2 mg, 36%. IR [KBr (cm^{-1})]: (ν_{B-F}) 1061 (s). ^1H NMR (400 MHz): δ = 7.34 (m, 18 H,

CH_{ar}), 4.57 (m, 4 H, CH_2–C_6H_5), 3.87 (m, 2 H, CH), 3.68 (m, 4 H, CH_2), 3.6 (m, 4 H, CH cod), 2.4 (m, 2 H, CH_2 cod), 2.1 (m, 1 H, CH_2 cod), 1.99 (m, 1 H, CH_2 cod), 1.58 (m, 2 H, CH_2 cod), 1.46 (m, 2 H, CH_2 cod) ppm. $^{13}C\{^1H\}$ NMR (100 MHz): δ = 137.67 (Ci), 134.68 (C_o–S), 129.79 (Ci-S), 129.14 (C_o), 128.87 (C_p), 128.79 (C_m), 117.63 (C_m-S), 76.43 (CH), 74.68 (CH cod), 73.87 (CH_2–C_6H_5), 73.74 (CH cod), 31.38 (CH_2 cod), 31.34 (CH_2 cod), 31.05 (CH_2) ppm. ^{19}F NMR (376 MHz, –60 °C): δ = –108.0 (m, **6c-I**), –113.89 (m, **6c-II**) ppm; **6c-I/6c-II** = 10:9.1. FAB$^+$: *m/z* (%) = 823 (M–BF_4). $C_{38}H_{40}BF_6IrO_2S_2$ (909.88): calcd. C 50.16, H 4.43, S 7.05; found C 49.69, H 4.43, S 7.13.

[Ir(cod)(1d)]BF_4 (6d): Colour: yellow; yield: 38.9 mg, 47%. IR [KBr (cm^{-1})]: (ν_{B-F}) 1063(s). ^1H NMR (400 MHz): δ = 7.42 (m, 20 H, H_{ar}), 4.62 (m, 4 H, CH_2–C_6H_5), 3.95 (m, 2 H, CH), 3.69 (m, 4 H, CH_2), 3.62 (m, 4 H, CH cod), 2.11 (m, 2 H, CH_2 cod), 1.98 (m, 2 H, CH_2 cod), 1.58 (m, 2 H, CH_2 cod), 1.47 (m, 2 H, CH_2 cod) ppm. $^{13}C\{^1H\}$ NMR (100 MHz): δ = 137.47 (Ci), 132.34 (Ci-S), 130.47 (C_o), 129.58 (C_o–S), 129.2 (C_m-S), 128.97 (C_p, C_p-S), 128.85 (C_m), 76.22 (CH), 74.84 (CH cod), 74.17 (CH cod), 73.82 (CH_2–C_6H_5), 31.39 (CH_2 cod), 31.33 (CH_2 cod), 29.74 (CH_2) ppm. FAB$^+$: *m/z* (%) = 787 (M–BF_4). $C_{38}H_{42}BF_4IrO_2S_2$ (873.9): calcd. C 52.23, H 4.84, S 7.34; found C 52.75, H 4.84, S 7.27.

[Ir(cod)(2b)]BF_4 (7b): Colour: yellow; yield: 53 mg, 86%. IR [KBr (cm^{-1})]: (ν_{B-F}) 1085 (s), (ν_{B-F}) 1055 (s). ^1H NMR (400 MHz): 7.26 (m, 18 H, H_{ar}), 4.23 (m, 2 H, CH), 4.05 (m, 4 H, CH cod), 3.54 (m, 4 H, CH_2), 2.25 (m, 4 H, CH_2 cod), 1.76 (m, 4 H, CH_2 cod), 1.42 (s, 6 H, CH_3) ppm. $^{13}C\{^1H\}$ NMR (100 MHz): δ = 161.0 (Ci-F, $J_{C,F}$ = 250.3), 132.17 (C_m), 130.17 (Ci), 127.03 (C_p-F), 118.11 (C_p), 117.88 (C_o–S), 111.90 ($C(CH_3)_2$), 80.57 (CH cod), 80.31 (CH cod), 78.52 (CH), 40.22 (CH_3), 31.56 (CH_2 cod), 27.22 (CH_2) ppm. ^{19}F NMR (376 MHz, –80 °C): δ = –108.3 (m, **7b-I**), –111.41 (m, **7b-II**) ppm; **7b-I/7b-II** = 10:3.8. $\Delta H^{\neq}$ = 16.4 ± 1 kJ mol^{-1}, $\Delta S^{\neq}$ = –0.1 kJ mol^{-1} K^{-1}, $\Delta G^{\neq}_{298.15}$ = 50.4 ± 1 kJ mol^{-1}. FAB+: *m/z* (%) = 683 (M–BF_4).

[Ir(cod)(2c)]BF_4 (7c): Colour: yellow; yield: 50.5 mg, 82%. IR [KBr (cm^{-1})]: (ν_{B-F}) 1084 (s), (ν_{B-F}) 1057 (s). ^1H NMR (400 MHz) 7.62 (m, 4 H, H_{ar}), 7.19 (m, 4 H, H_{ar}), 4.2 (m, 2 H, CH), 3.96 (m, 4 H, CH cod), 3.66 (m, 2 H, CH_2), 3.47 (m, 2 H, CH_2), 2.25 (m, 4 H, CH_2 cod), 1.77 (m, 4 H, CH_2 cod), 1.41 (s, 6 H, CH_3) ppm. $^{13}C\{^1H\}$ NMR (100 MHz): δ = 163.89 (Ci-F, $J_{C,F}$ = 249.5), 134.06 (C_o, $^3J_{C,F}$ = 6.3), 130.16 (Ci-S, $^4J_{C,F}$ = 2.3), 117.54 (C_m, $^2J_{C,F}$ = 16.6), 111.12 ($C(CH_3)_2$), 79.72 (CH cod), 79.78 (CH cod), 78.59 (CH), 40.61 (CH_3), 31.53 (CH_2 cod), 31.23 (CH_2) ppm. ^{19}F NMR (376 MHz, –80 °C): δ = –107.41 (m, **7c-I**), –115.62 (m, **7c-II**) ppm; **7c-I/7c-II** = 10:3.5. $\Delta H^{\neq}$ = 19.4 ± 1.3 kJ mol^{-1}, $\Delta S^{\neq}$ = –0.1 kJ mol^{-1} K^{-1}, $\Delta G^{\neq}_{298.15}$ = 48.1 ± 1.3 kJ mol^{-1}. FAB$^+$: *m/z* (%) = 683 (M–BF_4).

Procedure B: A solution of the corresponding ligand (**3**, **4**, 0.08 mmol) in dichloromethane (3 mL) was added to a solution of [Ir(cod)$_2$]BF_4 (40 mg, 0.08 mmol) in dichloromethane (5 mL) under nitrogen. After stirring for 40 min, the colour of the solution turned yellow-orange. The volume was reduced, and hexane was added to precipitate the product, which was collected by filtration, washed with additional hexane and vacuum dried.

[Ir(cod)(3)]BF_4 (8): Colour: yellow-orange; yield: 39.9 mg, 82%. IR [KBr (cm^{-1})]: (ν_{B-F}) 1054 (s). ^1H NMR (400 MHz, –80 °C, refer to Figure 3 for assignments): δ = 4.87 (m, 1 H, CH_a cod), 4.64 (m, 1 H, CH_d cod), 4.64 (m, 1 H, CH *5*), 4.50 (m, 1 H, CH_b cod) 4.45 (m, 1 H, CH_c cod), 4.14 (m, 1 H, CH *4*), 3.77 (m, 1 H, CH_2 *3*), 3.59 (m, 1 H, CH_2 *6*), 3.28 (m, 3 H, CH_2 *6′,1, 2′*), 3.07 (m, 1 H, CH_2 *2*), 2.82 (m, 1 H, CH_2 *1′*), 2.58 (m, 1 H, CH_2 *3′*) 2.17 (m, 4 H, CH_2 cod), 2.02 (m, 2 H, CH_2 cod), 1.89 (m, 2 H, CH_2 cod), 1.34 (s, 3 H, CH_3), 1.36 (s, 3 H, CH_3) ppm; (20 °C): δ = 4.95 (m, 1 H, CH_a cod), 4.75 (m, 1 H, CH_d cod), 4.68 (m, 1, CH *5*), 4.61 (m, 1 H, CH_b cod) 4.44 (m, 1 H, CH_c cod), 4.19 (m, 1 H, CH *4*), 3.83 (m, 1 H, CH_2 *3*), 3.62 (m, 1 H, CH_2 *6*), 3.36 (m, 3 H, CH_2 *6′,1, 2′*), 3.17 (m, 1 H, CH_2 *2*), 2.89 (m, 1 H, CH_2 *1′*), 2.61 (m, 1 H, CH_2 *3′*) 2.26 (m, 4 H, CH_2 cod), 2.05 (m, 4 H, CH_2 cod), 1.41 (s, 6 H, CH_3) ppm. $^{13}C\{^1H\}$ NMR (100 MHz): δ = 111.09 ($C(CH_3)_2$), 83.43 (CH_a cod), 83.14 (CH, *5*), 81.29 (CH_d cod), 78.61 (CH_b cod), 76.73 (CH_c cod), 76.31 (CH, *4*), 46.54 (CH_2 *6*), 41.04 (CH_2 *3*), 36.55 (CH_2 *2*), 33.08 (CH_2 *1*), 32.41 (CH_2 cod), 32.11 (CH_2 cod), 31.66 (CH_2 cod), 31.34 (CH_2 cod), 28.56 (CH_3) ppm. FAB$^+$: *m/z* (%) = 521 (M–BF_4). High resolution FAB$^+$: *m/z* (%) = 521.1226; $C_{17}H_{28}IrO_2S_2$ (Err [ppm/mmu] = +12.7/+6.6). $C_{17}H_{28}BF_4IrO_2S_2$ (607.56): calcd. C 33.61, H 4.65, S 10.56; found C 33.71, H 4.63, S 10.60.

[Ir(cod)(4)]BF_4 (9): Colour: yellow-orange; yield: 49.3 mg, 99%. IR [KBr (cm^{-1})]: (ν_{B-F}) 1053 (s). ^1H NMR (300 MHz, refer to Figure 3 for assignments): δ = 4.91 (m, 1 H, CH *5*), 4.61 (m, 1 H, CH_a CH_a CH_a CH_a cod), 4.58 (m, 1 H, CH *6*), 4.93 (m, 1 H, CH_d cod), 4.21 (m, 1 H, CH_b cod), 4.06 (m, 1 H, CH_c cod), 3.75 (m, 1 H, CH_2 *7′*), 3.54 (m, 1 H, CH_2 *4*), 3.46 (m, 2 H, CH_2 *1,3*), 3.44 (m, 1 H, CH_2 *4′*), 3.24 (m, 2 H, CH_2 *2,2′*), 3.0 (m, 2 H, CH_2 *1,3*), 2.71 (m, CH_2 *7*), 2.40–2.19 (m, 8 H, CH_2 cod), 1.43 (s, 6 H, CH_3) ppm. $^{13}C\{^1H\}$ NMR (75 MHz): δ = 106.06 ($C(CH_3)_2$), 79.31 (CH_a cod), 78.46 (CH, *5*), 77.94 (CH_d cod), 73.84 (CH_b cod), 73.71 (CH_c cod), 72.04 (CH, *6*), 38.28 (CH_2, *7*), 34.09 (CH_2 *4*), 30.09 (CH_2 *2*), 28.57 (CH_2 *1*), 27.7 (CH_2, cod), 27.03 (CH_2 cod), 26.71 (CH_2 cod), 24.96 (CH_2 *3*), 24.62 (CH_2 cod) 22.24 (CH_3), 21.90 (CH_3) ppm. FAB$^+$: *m/z* (%) = 535 (M–BF_4). High resolution FAB$^+$: *m/z* (%) = 535.1344; $C_{18}H_{30}IrO_2S_2$ (Err [ppm/mmu] = +5.1/+2.7).

Procedure C: The corresponding ligand (**5a**,**b**, 0.12 mmol) was added to a solution of [Ir(cod)$_2$]BF_4 (40 mg, 0.08 mmol) in dichloromethane (5 mL) under nitrogen. After stirring for 30 min, the colour of the solution turned yellow-orange. Diethyl ether was added to precipitate the product, which was collected by filtration, washed with additional diethyl ether and vacuum dried.

[Ir(cod)(5a)]BF_4.CH_2Cl_2 (10a.CH_2Cl_2): Colour: yellow; yield: 29.2 mg, 48%. ^1H NMR ($CDCl_3$, 300 MHz): δ = 7.7 (m, 10 H, C_6H_5), 4.0 (m, 6 H, CH + CH cod), 2.4 (t, 2 H, CH_2, $J_{H,H}$ = 5.1 Hz), 2.28 (m, 4 H, CH_2 cod), 1.8 (m, 4 H, CH_2 cod), 1.48 (d, 6 H, CH_3, $J_{H,H}$ = 6.3 Hz) ppm. $^{13}C\{^1H\}$ NMR ($CDCl_3$, 75 MHz): δ = 133.68 (C*o*), 131.78 (C*m*), 130.38 (C*p*), 79.06 (CH cod), 78.52 (CH cod), 44.17 (CH), 38.83 (CH_2), 31.58 (CH_2 cod), 30.75 (CH_2 cod), 20.57 (CH_3) ppm. FAB$^+$: *m/z* (%) = 589 (M–BF_4). $C_{25}H_{32}BF_4IrS_2$·CH_2Cl_2 (760.63): calcd. C 41.06, H 4.51, S 8.44; found C 41.30, H 4.70, S 8.04.

[Ir(cod)(5b)]BF_4 (10b): Colour: orange; yield: 26.7 mg, 55%. ^1H NMR ($CDCl_3$, 300 MHz,): δ = 4.37 (m, 2 H, CH cod), 4.13 (m, 2 H, CH cod), 3.76 (sextuplet, 2 H, CH, $J_{H,H}$ = 5.4 Hz), 3.55 (sept, 2 H, *i*Pr CH, $J_{H,H}$ = 6.9 Hz), 2.56 (t, 2 H, CH_2, $J_{H,H}$ = 5.4 Hz), 2.3 (m, 4 H, CH cod), 2.02 (m, 2 H, CH_2 cod), 1.78 (m, 2 H, CH cod), 1.61 (d, *i*Pr CH_3, $J_{H,H}$ = 6.6 Hz), 1.54 (d, 6 H, *i*Pr CH_3, $J_{H,H}$ = 6.4 Hz) 1.53 (d, 6 H, *i*Pr CH_3, $J_{H,H}$ = 6.5 Hz) ppm. $^{13}C\{^1H\}$ NMR ($CDCl_3$, 75 MHz): δ = 78.24 (CH cod), 75.39 (CH cod), 41.53 (CH_2), 41.0 (CH), 40.06 (*i*Pr CH), 32.75 (CH_2 cod), 30.42 (CH_2 cod), 24.20 (CH_3), 23.26 (*i*Pr CH_3), 22.84 (*i*Pr CH_3) ppm. FAB$^+$: *m/z* (%) = 521 (M–BF_4). $C_{19}H_{36}BF_4IrS_2$ (607.65): calcd. C 37.56, H 5.97, S 10.55; found C 37.98, H 6.57, S 10.91.

Synthesis of [Ir(H)$_2$(cod)(dithioether)]BF_4 (dithioether = 3, 4)

General Procedure: Hydrogen was bubbled into an NMR tube containing a solution of [Ir(cod)(dithioether)]BF_4 (ditihioether = **3**, **4**)

(0.066 mmol) in deuterated dichloromethane at –72 °C for 20 min, obtaining yellow solutions in both cases. The tube was introduced into the NMR equipment at –80 °C and spectra were acquired. The relaxation time, T_1, was determined at –70 °C, and then the temperature was increased by 10 °C intervals, recording spectra at each successive temperature, until 25 °C was reached. 2D NMR spectra were acquired at 25 °C for complex $[Ir(H)_2(cod)(\mathbf{3})]BF_4$ and at 0 °C for complex $[Ir(H)_2(cod)(\mathbf{4})]BF_4$.

$[Ir(H)_2(cod)(3)]BF_4$ (13): ^{1}H NMR (300 MHz, –70 °C, refer to Figure 3 and Figure 7 for assignments): δ = 4.85 (m, 1 H, CH_a cod), 4.64 (m, 1 H, CH_d cod), 4.50 (m, 1, CH *5*), 4.41 (m, 1 H, CH_b cod) 4.41 (m, 1 H, CH_c cod), 4.13 (m, 1 H, CH *4*), 3.77 (m, 1 H, CH_2 *3*), 3.59 (m, 1 H, CH_2 *6*), 3.28 (m, 3 H, CH_2 *6′,1, 2′*), 3.07 (m, 1 H, CH_2 *2*), 2.80 (m, 1 H, CH_2 *1′*), 2.59 (m, 1 H, CH_2 *3′*) 2.06 (m, 4 H, CH_2 cod), 1.91 (m, 4 H, CH_2 cod), 1.34 (s, 3 H, CH_3), 1.33 (s, 3 H, CH_3), –11.37 [s, 1 H, complex **13-I**, H*f*, T_1 = 0.3112 s (err = 0.008368)], –11.56 [s, 1 H, complex **13-II**, H*f*, T_1 = 0.3112 s (err = 0.009975)], –13.78 [s, 1 H, complex **13-II**, H*e*, T_1 = 0.222 s (err = 0.006233)], –13.83 [s, 1 H, complex **13-I**, H*e*, T_1 = 0.2087 s (err = 0.003677)] ppm; **13-I/13-II** = 5:3. ^{1}H NMR (CD_2Cl_2, 300 MHz, 20 °C): δ = 4.93 (m, 1 H, CH_a cod), 4.76 (m, 1 H, CH_d cod), 4.66 (m, 1, CH *5*), 4.60 (m, 1 H, CH_b cod) 4.43 (m, 1 H, CH_c cod), 4.17 (m, 1 H, CH *4*), 3.81 (m, 1 H, CH_2 *3*), 3.34 (m, 1 H, CH_2 *6*), 3.316 (m, 3 H, CH_2 *6′,1, 2′*), 3.15 (m, 1 H, CH_2 *2*), 2.91 (m, 1 H, CH_2 *1′*), 2.61 (m, 1 H, CH_2 *3′*) 2.24 (m, 4 H, CH_2 cod), 2.06 (m, 4 H, CH_2 cod), 1.39 (s, 6 H, CH_3), –11.39 (s, 1 H, complex **1**, H*f*), –11.59 (s, 1 H, complex **2**, H*f*), –13.87 (s, 1 H, complex **2**, H*e*), –13.85 (s, 1 H, complex **1**, H*e*) ppm.

$[Ir(H)_2(cod)(4)]BF_4$ (14): ^{1}H NMR (400 MHz, 0 °C, refer to Figure 3 for assignments): δ = 4.91 (m, 1 H, CH *5*), 4.6 (m, 2 H, CH_a cod + CH *6*), 4.94 (m, 1 H, CH_d cod), 4.18 (m, 1 H, CH_b cod), 4.07 (m, 1 H, CH_c cod), 3.76 (m, 1 H, CH_2 *7′*), 3.57 (m, 1 H, CH_2 *4*), 3.38 (m, 2 H, CH_2 *1,3*), 3.35 (m, 1 H, CH_2 *4′*), 3.29 (m, 2 H, CH_2 *2, 2′*), 3.03 (m, 2 H, CH_2 *1, 3*), 2.78 (m, CH_2 *7*), 2.38–1.91 (m, 8 H, CH_2 cod), 1.43, 1.41 (s, 6 H, CH_3, *0.5:1*), –12.57 [s, 1 H, complex **14-I/II**, H*f*, T_1 = 0.4089 s (err = 0.01158)], –12.72 [s, 1 H, complex **14-I/II**, H*f*, T_1 = 0.3934 s (err = 0.009862)], –12.84 [s, 1 H, complex **14-I/II**, H*e*, T_1 = 0.2825 s, (err = 0.009123)], –13.28 [s, 1 H, complex **14-I/II**, H*e*, T_1 = 0.2846 s (err = 0.007316)] ppm.

Catalysis: A standard hydrogenation experiment was performed in the following manner.[25] A solution in dichloromethane (6 mL) containing the complex $[Ir(cod)L]BF_4$ (L = dithioether or cod, 0.026 mmol) and the substrate (1.05 mmol) was introduced into the evacuated hydrogenation system which was filled up to atmospheric pressure with hydrogen. The mixture was vigorously stirred using a wrist-shaker and it was analysed directly by GC in the case of substrates **11a** and **11c**. The final mixtures resulting from the hydrogenation of acid substrates **11b** and **11d** were transformed into the esters by the following procedure: trimethylsilyldiazomethane (0.3 mL, 2 M in hexane) and MeOH (0.1 mL) were added to the final catalytic solution (0.5 mL). This mixture was stirred for 30 min at room temperature, filtered through silica and analysed by GC.

Crystal Data for Complex 10b: Suitable crystals of complexes **10b** were grown by slow diffusion of *n*-hexane into a solution of the complex in ethyl acetate and mounted on a glass fiber. The X-ray data were collected at 293.5 K with a Bruker APEX instrument (Mo-K_α radiation, λ = 0.71073 Å). The SHELXTL v. 6.1 program package was used for structure solution and refinement. An absorption correction was applied using SADABS. The structure was solved by direct methods and refined by full-matrix least-squares procedures. All non-hydrogen atoms were refined anisotropically. $C_{19}H_{36}BF_4IrS_2$, M = 607.61, Monoclinic space group $P2_1$, a = 9.2855(12), b = 12.5844(17), c = 10.0187(13) Å, β = 97.892(2)°, V = 1159.6(3) Å^3, Z = 2, D_c = 1.740 Mg/m^3, 11295 reflections measured, 4057 unique (R_{int} = 0.0492) which were used in all calculations; the final R value was 0.0331 [$F > 4\sigma(F)$] and 0.0501 (all data). The ORTEP diagram was generated using ORTEP-3.[50]

CCDC-239321 contains the supplementary crystallographic data for this paper. These data can be obtained free of charge from The Cambridge Crystallographic Data Centre via www.ccdc.cam.ac.uk/data_request/cif.

Acknowledgments

This work was financially supported by CONACyT from Mexico (Ref. 34982), and Ministerio de Educación y Cultura from Spain (PB97-0407-C05-01 and PB98-0641). L. F.-S. appreciates the fellowship of DGEP-UNAM and CONACyT.

[1] J. C. Bayón, C. Claver, A. M. Masdeu-Bultó, *Coord. Chem. Rev.* **1999**, *193–195*, 73–195.
[2] A. M. Masdeu-Bultó, M. Diéguez, E. Martin, M. Gómez, *Coord. Chem. Rev.* **2003**, *242*, 159–201.
[3] P. Barbaro, A. Currao, H. Jörg, R. Nesper, P. S. Pregosin, R. Salzmann, *Organometallics* **1996**, *15*, 1879–1888.
[4] M. Hiraoka, A. Mishikawa, T. Marimoto, K. Achiwa, *Chem. Pharm. Bull.* **1998**, *46*, 704–706.
[5] E. Hauptman, P. J. Fagan, W. Marshall, *Organometallics* **1999**, *18*, 2061–2073.
[6] O. Pámies, M. Diéguez, G. Net, A. Ruiz, C. Claver, *Organometallics* **2000**, *19*, 1488–1496.
[7] A. Albinati, P. S. Pregosin, K. Wick, *Organometallics* **1996**, *15*, 2419–2421.
[8] D. A. Evans, K. R. Campos, J. S. Tedrow, F. E. Michael, M. R. Gagné, *J. Am. Chem. Soc.* **2000**, *122*, 7905–7920.
[9] K. Boog-Wick, P. S. Pregosin, G. Trabesinger, *Organometallics* **1998**, *17,* 3254–3264.
[10] S.-L. You, X.-L. Hou, L.-X. Dai, Y.-H. Yu, W. Xia, *J. Org. Chem.* **2002**, *67*, 4684–4695.
[11] B. K. Vriesema, M. Lemaire, J. Buter, R. M. Kellog, *J. Org. Chem.* **1986**, *51*, 5169–5177.
[12] C. G. Frost, J. M. J. Williams, *Tetrahedron: Asymmetry* **1993**, *4,* 1785–1788.
[13] C. G. Frost, G. Christopher, J. M. J. Williams, *Tetrahedron Lett.* **1993**, *34*, 2015–2018.
[14] G. J. Dawson, C. G. Frost, C. J. Martin, J. M. J. Williams, S. J. Coote, *Tetrahedron Lett.* **1993**, *34,* 7793–7795.
[15] J. V. Allen, J. F. Bower, J. M. J. Williams, *Tetrahedron: Asymmetry* **1994**, *5*, 1895–1898.
[16] J. V. Allen, S. J. Coote, G. J. Dawson, C. G. Frost, C. J. Martin, J. M. J. Williams, *J. Chem. Soc. Perkin Trans. 1* **1994**, 2065–2072.
[17] H. Adams, J. C. Anderson, R. Cubbon, D. S. James, J. P. Mathias, *J. Org. Chem.* **1999**, *64*, 8256–8262.
[18] C. G. Frost, J. M. J. Williams, *Synlett* **1994**, *7*, 551–552.
[19] O. Pàmies, G. Net, A. Ruiz, C. Claver, S. Woodward, *Tetrahedron: Asymmetry* **2000**, *11*, 871–877.
[20] S. M. W. Bennett, S. M. Brown, A. Cunningham, M. R. Dennis, J. P. Muxworthy, M. A. Oakley, S. Woodward, *Tetrahedron* **2000**, *56*, 2847–2855.
[21] C. Börner, M. R. Dennis, E. Sinn, S. Woodward, *Eur. J. Org. Chem.* **2001**, 2435–2446.
[22] C. Börner, W. A. König, S. Woodward, *Tetrahedron Lett.* **2001**, *42*, 327–329.
[23] D. A. Evans, F. E. Michael, J. S. Tedrow, K. R. Campos, *J. Am. Chem. Soc.* **2003**, *125*, 3534–3543.
[24] S. Jansat, M. Gómez, G. Muller, M. Diéguez, A. Aghmiz, C. Claver, A. M. Masdeu-Bultó, L. Flores-Santos, E. Martin,

M. A. Maestro, J. Mahía, *Tetrahedron: Asymmetry* **2001**, *12*, 1469–1474.
[25] M. Diéguez, A. Orejón, A. M. Masdeu-Bultó, R. Echarri, S. Castillón, C. Claver, A. Ruiz, *J. Chem. Soc. Dalton Trans.* **1997**, 4611–4618.
[26] M. Diéguez, A. Ruiz, C. Claver, M. M. Pereira, A. M. d′A. Rocha Gonsalves, *J. Chem. Soc. Dalton Trans.* **1998**, 3517–3522.
[27] N. Ruiz, A. Aaliti, J. Forniés-Cámer, A. Ruiz, C. Claver, C. J. Cardin, D. Fabbri, S. Gladiali, *J. Organomet. Chem.* **1997**, *545*, 79–87.
[28] O. Pàmies, M. Diéguez, G. Net, A. Ruiz, C. Claver, *J. Chem. Soc. Dalton Trans.* **1999**, 3439–3444.
[29] D. Enders, R. Peters, R. Lochtman, G. Raabe, J. Runsink, J. W. Bats, *Eur. J. Org. Chem.* **2000**, 3399–3426.
[30] W. Li, J. P. Waldkirch, X. Zhang, *J. Org. Chem.* **2002**, *67*, 7618–7623.
[31] N. Khiar, C. S. Araujo, E. Alvarez, I. Fernández, *Tetrahedron Lett.* **2003**, *44*, 3401–3404.
[32] R. Siedlecka, E. Wojaczyńska, J. Skarżewski, *Tetrahedron: Asymmetry* **2004**, *15*, 1437–1444.
[33] L. Flores-Santos, E. Martin, M. Diéguez, A. M. Masdeu-Bultó, C. Claver, *Tetrahedron: Asymmetry* **2001**, *12*, 3029–3034.
[34] F. Fernández, M. Gómez, S. Jansat, G. Muller, L. Flores-Santos, A. Acosta-Ramirez, P. García-Reynaldos, E. Martin, A. Aghmiz, M. Giménez-Pedrós, M. Diéguez, C. Claver, A. M. Masdeu-Bultó, M. A. Maestro, *Organometallics*, in preparation.
[35] Calculated by gNMR software (P. H. M. Budzelaar, Cherwell Scientific Publishing, **1995**–**1997**).
[36] E. W. Abel, S. K. Bhargava, K. G. Orrell in *Progress in Inorganic Chemistry* (Ed.: S. J. Lippard), John Wiley & Sons, **1984**, vol. 32, p. 1.
[37] K. G. Orrell, *Coord. Chem. Rev.* **1989**, *96*, 1–48.
[38] S. O. Grim, P. B. Kettler, J. S. Merola, *Inorg. Chim. Acta* **1991**, *185*, 57–61.
[39] M. Abbas, P. A. Chaloner, C. Claver, P. Hitchcock, A. M. Masdeu, A. Ruiz, T. Saballs, *J. Organomet. Chem.* **1991**, *403*, 229.
[40] H. A. Jenkins, S. J. Loeb, *Organometallics* **1994**, *13*, 1840–1850.
[41] A. J. Blake, M. A. Halcrow, M. Schröder, *J. Chem. Soc. Chem. Commun.* **1991**, 253–256.
[42] F. A. Cotton, P. Lahuerta, J. Latorre, M. Sanaú, I. Solana, W. Schwotzer, *Inorg. Chem.* **1988**, *27*, 2131–2135.
[43] E. Fernández, A. Ruiz, S. Castillón, C. Claver, J. F. Piniella, A. Alvarez-Larena, G. Germain, *J. Chem. Soc. Dalton Trans.* **1995**, 2137–2142.
[44] G. J. Kubas, *Acc. Chem. Res.* **1988**, *21*, 120–128.
[45] D. G. Hamilton, R. H. Crabtree, *J. Am. Chem. Soc.* **1988**, *110*, 4126–4133.
[46] P. J. Desrosiers, L. Cai, Z. Lin, R. Richards, J. Halpern, *J. Am. Chem. Soc.* **1991**, *113*, 4173–4184.
[47] R. H. Crabtree, *Angew. Chem. Int. Ed. Engl.* **1993**, *32*, 789–805.
[48] D. M. Heinekey, A. Liegeois, M. van Room, *J. Am. Chem. Soc.* **1994**, *116*, 8388–8389.
[49] M. Green, T. A. Kuc, S. H. Taylor, *J. Chem. Soc. A* **1971**, 2334–2337.
[50] *ORTEP-3 for Windows*: L. J. Farrugia, *J. Appl. Crystallogr.* **1997**, *30*, 565–565.

Received: October 5, 2004

